COHERENCE LENGTH AND HOLOGRAPHY

T. H. Jeong, Q. Feng, E. Wesly, and Z. Qu

Center for Photonics Studies
Department of Physics
Lake Forest College
Lake Forest, IL 60045

1. Abstract

The development of the field of holography has depended on the coherence of laser light. The most meaningful attribute of coherence for holographers is the coherence length. Commonly, coherence length is regarded as the maximum optical path difference between two beams, such as those in a Michelson interferometer, that results in a discernable interference pattern. Herein we discuss two direct holographic methods of measuring coherence length, each yielding visually observable results. We begin by examining several theoretical models for laser spectral line-widths and the corresponding derivation of coherence lengths.

2. Spectroscopy and Line Shape

Let us first discuss some basic characteristics of laser spectroscopy, since it leads us directly to the understanding of coherence.

When studying the intensity of laser output with respect to laser frequency, it is found that each spectral line consists of an intrinsic spectral distribution about the line center. The profile of each spectral line has a finite width and a characteristic shape which are determined by the conditions of the source. The output is not strictly monochromatic (single frequency), but rather broadened for various reasons. The line profile is important in determining many of the characteristics of gas lasers, especially its coherence length. We will briefly describe the line-broadening mechanisms.

I. The Natural Line Broadening

This is the intrinsic broadening of spectral lines of isolated atoms due to the finite life-time of excited states, also called the radiative broadening. The shape of the profile is Lorentzian and the broadening is homogeneous (has the same effect on all atoms).

(i) Classical Model

Classically, by introducing the radiation reaction force, it can be shown that the line shape of radiation from level E_i to level E_f is determined by (1)

$$I_{fi}(\omega) = I_0 \frac{\gamma/2\pi}{(\omega-\omega_{fi})^2+\gamma^2/4} \qquad (1)$$

where $\gamma = e^2\omega_{fi}^2/6\pi\varepsilon_0 c^3 m$, $\omega_{fi} = 2\pi(E_i-E_f)/h$, e and m are the charge and mass of electrons respectively, c is the speed of light; and the FWHM (full width at half maximum intensity) is

$$\Delta\omega_{1/2} = \gamma \tag{2}$$

which is the width predicted by the uncertainty principle.

(ii) Quantum-mechanical Model

According to the Weisskopf & Wigner's theory, the profile can also be described quantum mechanically (2)

$$I_{fi}(\omega) = I_0 \frac{\Gamma_{fi}/2\pi}{(\omega - \omega_{fi})^2 + \Gamma_{fi}^2/4} \tag{3}$$

where $\Gamma_{fi} = \Gamma_f + \Gamma_i$, and Γ_f and Γ_i are the radiative life-times of the final and initial levels, respectively. The FWHM is given by

$$\Delta\omega_{1/2} = \Gamma_{fi} \tag{4}$$

The natural width of spectral lines is generally small in comparison to other contributions of line broadening, but it does set a theoretical limit to the width of spectral lines.

II. The Pressure Line Broadening

The interaction forces between neighboring atoms, ions or electrons affect the shape of the spectral lines and lead to a broadening of the line that is usually wider than its natural width. This broadening is also Lorentzian and homogeneous. There are two approximations commonly used in describing its profiles: the quasi-static approximation is suitable for high densities and low temperatures, while the impact approximation is suitable for low pressure and high temperatures.

III. The Doppler Line Broadening

This broadening effect is due to the random thermal motion of the emitting atoms. It dominates the shape and the width of spectral lines in the ultraviolet and visible region of the spectrum. It has a Gaussian profile and is inhomogeneous.

The profile of a Doppler-broadened spectral line is given by the normalized Gaussian distribution with a FWHM of (3)

$$\Delta\nu_{1/2} = 2\frac{\nu_0}{c}\left(\frac{2kT}{M}\ln 2\right)^{1/2} = 7.16 * 10^{-7}\nu_0\left(\frac{T}{A}\right)^{1/2} \tag{5}$$

where k is the Boltzman constant, M is the mass of the radiating particle, A is the mass number of the radiating particle, T is the temperature of the source, ν_0 is the center frequency of the output.

A comparison of the natural, collisional, and Doppler broadenings shows that under normal conditions, Doppler broadening is about two orders of magnitude greater than the other two. (4)

IV. The Model of Spectral Density of Lasers

The spectral power distribution of laser output usually consists of several modes under some profile. Here we will study the various aspects of this distribution (Figure 1).

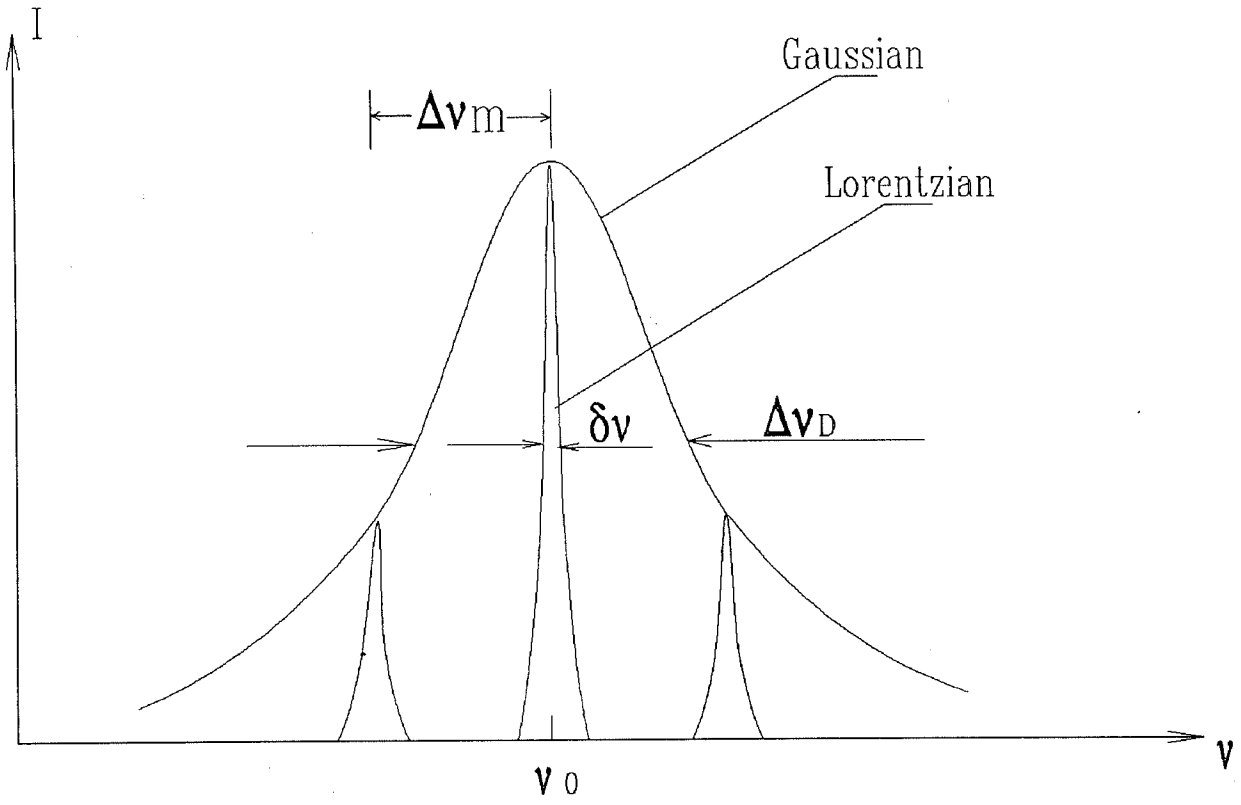

Figure 1

(i) Profile

The profile of the spectral density distribution is Gaussian, with FWHM $\Delta\nu_{1/2}$ given in Equation (5).

The range of the resonance modes of a laser is restricted by the frequency range over which the gain required for lasing is satisfied. However, we may assume that the gain conditions are sufficient to produce oscillation and we should be only concerned with the modes within a spectral profile.

(ii) The line shape of a single mode

The shape of each single mode may be described by an Airy function as in the case of a Fabry-Perot etalon. A Lorentzian function may be used as an approximation and will simplify the calculation significantly. The width of cavity resonance modes is limited by the Schawlow-Townes equation: (5)

$$\delta\nu = \frac{2\pi(\Delta\nu_m)^2 h\nu}{P} \tag{6}$$

where $\Delta\nu_m$ is the spacing between adjacent cavity modes, P is the output power. The line width of the modes is limited by the Q factor of the cavity, and has nothing to do with the source.

(iii) Positioning and Spacing of the modes

For the sake of simplicity, we will let all the modes within the Doppler profile be positioned symmetrically with respect to the center of the profile. This assumption is arbitrary, but it does not change the result significantly.

Spacing between adjacent modes is given by

$$\Delta \nu_m = \frac{c'}{2L} \tag{7}$$

where c' is the speed of light inside the cavity and L is the length of the cavity.

3. Simplified Models and Predictions

In order to calculate the coherence length of lasers, it is necessary to have some model of laser spectral density. Here we review some simplified models and their predictions about the coherent length.

I. An idealized model of the power spectral density of a gas laser with N equal-intensity axial modes (Figure 2)

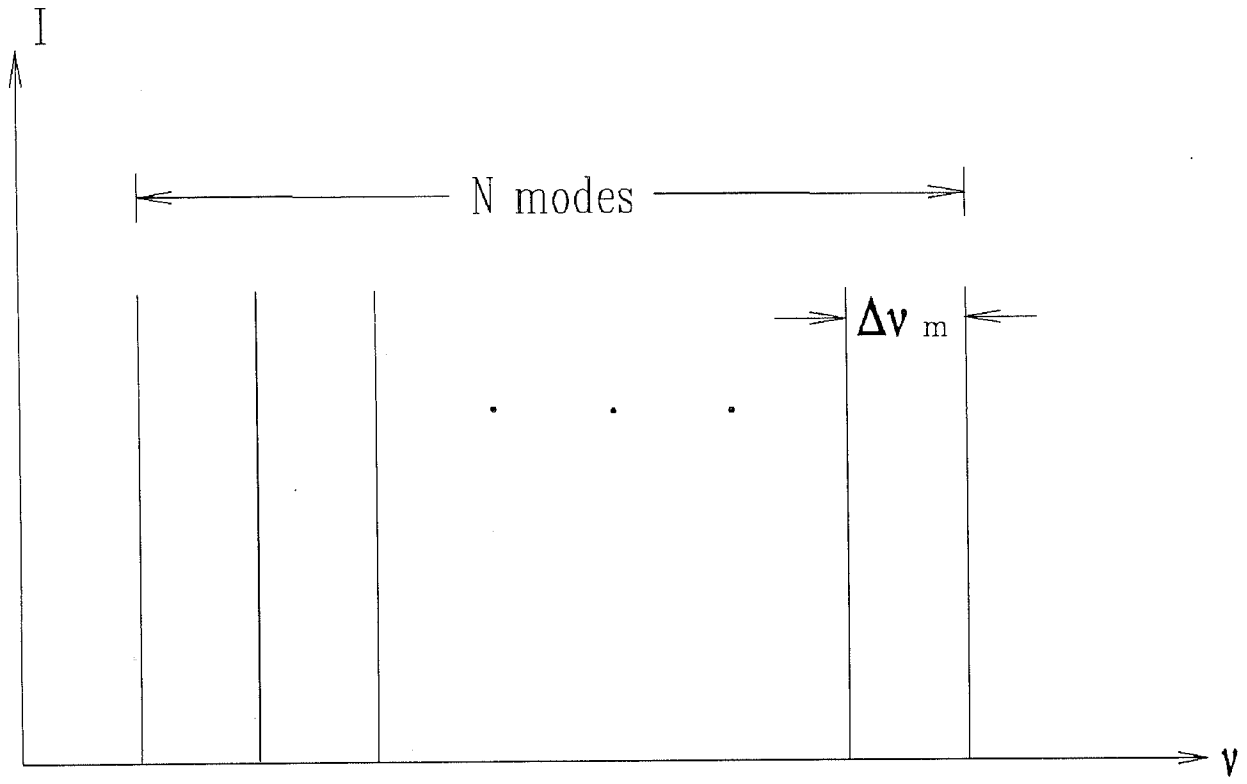

Figure 2

The famous uncertainty principle has a very deep relation with coherence length. This has to do with the unique behavior of photons (6). Here we will use one form of the uncertainty principle

$$\Delta t \Delta \nu = 1 \tag{8}$$

where $\Delta\nu$ is the variation in frequency and Δt is the least time needed to measure such variation. If $\Delta\nu$ is measured using a Michelson interferometer (as shown later in Figure 8), $c\Delta t$ is equal to the maximum path difference in the two arms of the interferometer. Any time period longer than Δt in Equation (8) will suffice to tell the frequency uncertainty $\Delta\nu$. Therefore Δt is directly related to coherent length l_{co} and may be called coherence time. Since

$$\Delta \nu = (N-1)\,\Delta \nu_m = (N-1)\frac{c'}{2L} \tag{9}$$

so we have

$$l_{co} = c\,\Delta t = c\frac{1}{\Delta \nu} = \frac{2L}{N-1}\frac{c}{c'} \tag{10}$$

Here the discrete modes have been treated the same as continuous spectral density.

II. δ-function modes within a Doppler profile (Figure 3)

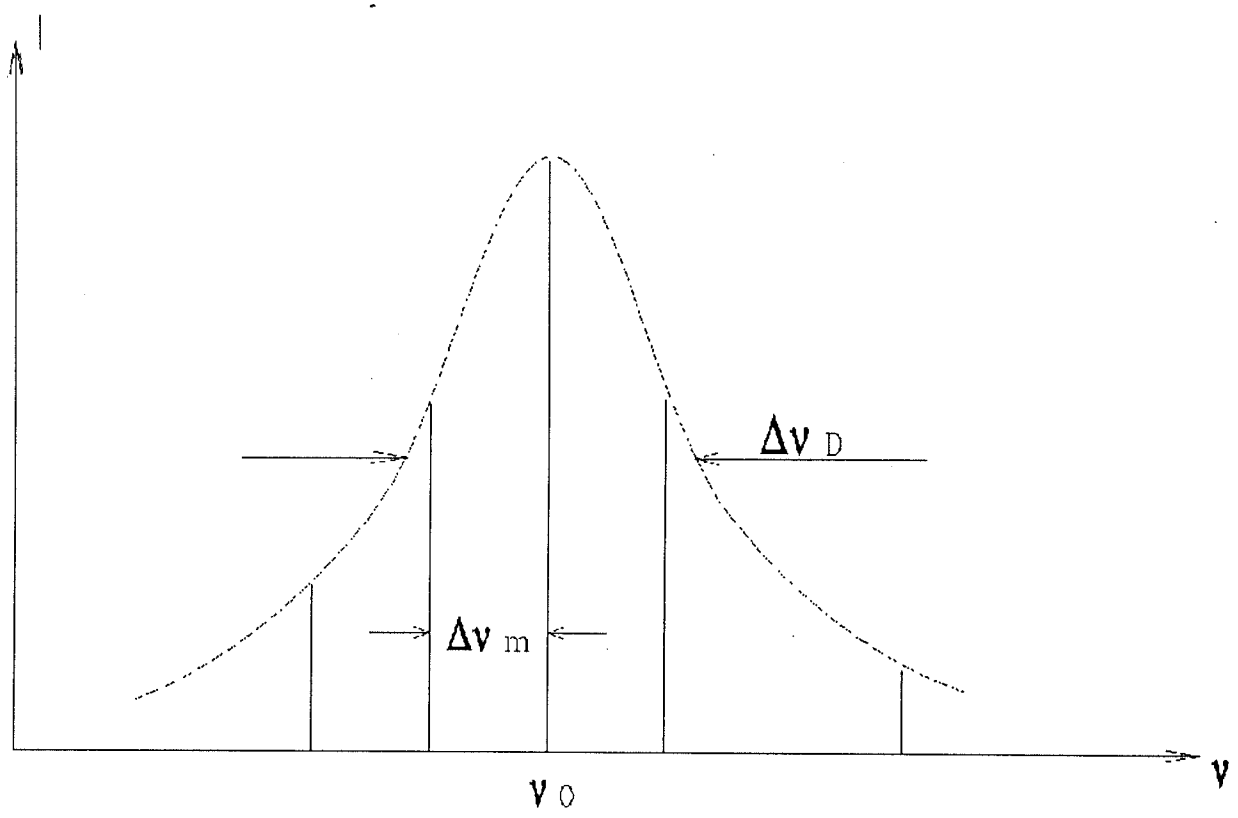

Figure 3

This model is a little more complicated than the above one and it takes into account the Doppler profile. Again using Equation (8), the coherent length is

$$l_{co} \approx \frac{c}{\Delta \nu_D} \tag{11}$$

where $\Delta\nu_D$, the width of the Doppler profile, is the same as $\Delta\nu_{1/2}$ calculated in Equation (5). It can also be written in the same form as (10) if N is considered the number of modes within the FWHM of the Doppler profile. Assuming c=c', we have

$$l_{co} = \frac{2L}{N-1} \tag{12}$$

Later we will see that this equation agrees well with the data. The Appendix at the end of this paper provides a geometric proof that yields the same result.

III. Continuous spectral density instead of discrete modes

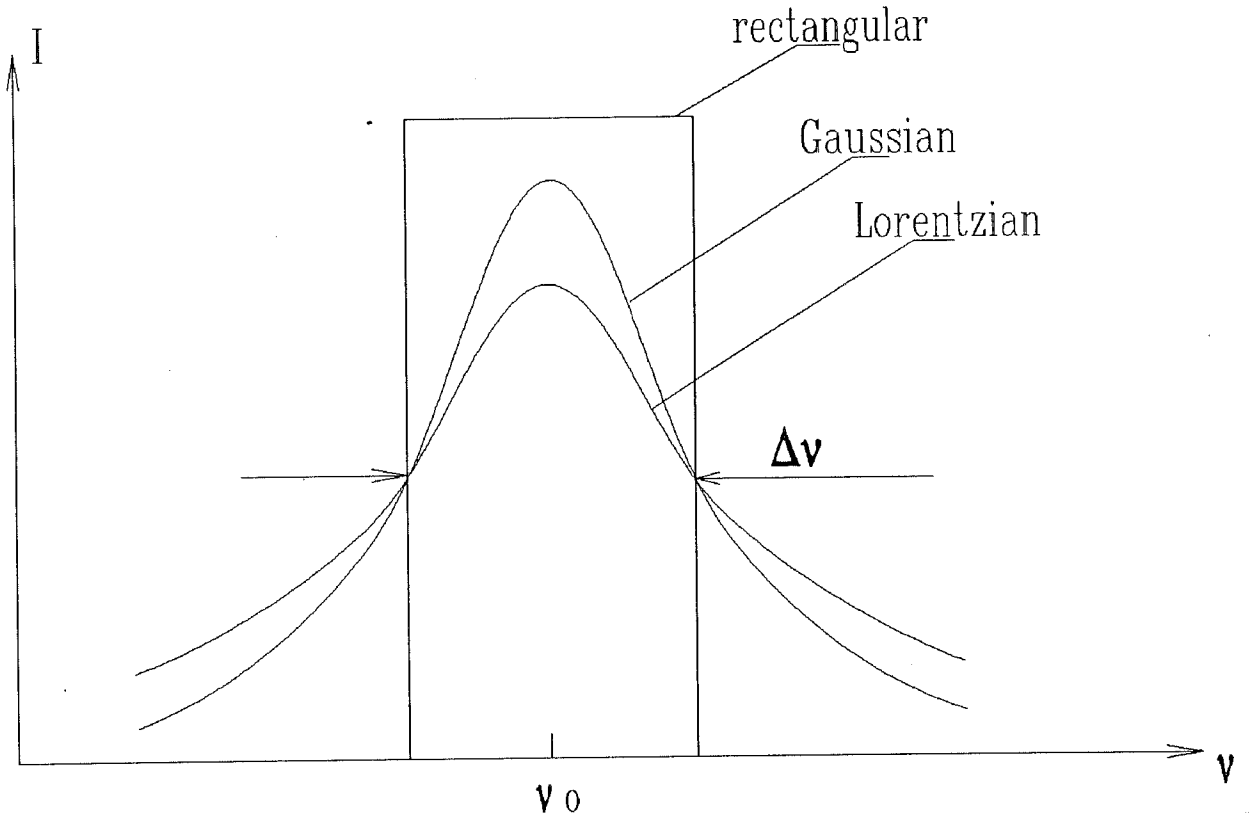

Figure 4

Various shapes of continuous spectral density are considered in Figure 4 (7). The corresponding coherence times are given as

$$\tau_c = \frac{0.664}{\Delta \nu} \qquad \textit{Gaussian} \tag{13}$$

$$\tau_c = 0.\frac{318}{\Delta\nu} \qquad \textit{Lorentzian} \tag{14}$$

$$\tau_c = \frac{1}{\Delta\nu} \qquad \textit{rectangular} \tag{15}$$

where $\Delta\nu$ is the FWHM in each case.

4. Experiments and Results

I. Experiments

Since we are mainly concerned with coherent length of lasers in hologram making, it is natural that we measure it by holographic means. In ordered to do this, we designed two setups.

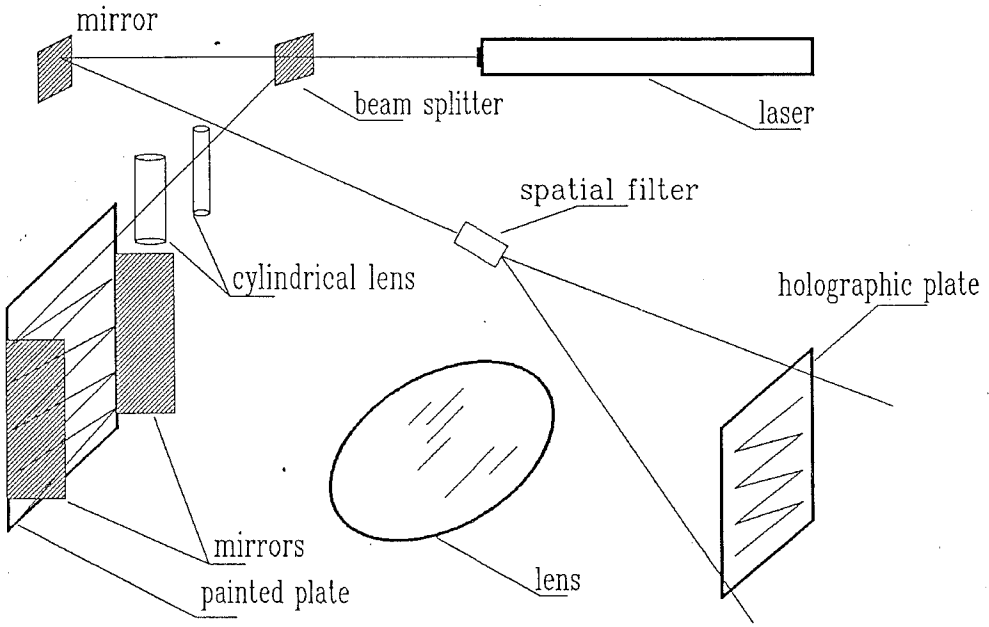

Figure 5

In Figure 5, laser beam goes through a beam splitter; part of it is expanded and then collimated in the horizontal direction by two cylindrical lenses (so that it is roughly plane wave) and goes on to a plate painted white. It is reflected back and forth between the two mirrors on both sides of the plate and leaves its trace on the plate. This trace is then focused onto the holographic plate through a lens (diameter 30 cm, f=50 cm). The zero path length point is carefully marked on the plate. The other part of the beam goes through a 40X spatial filter and interferes as a reference with the image of the plate at the focal plane. This produces white light viewable hologram of the path of the beam from which we can directly read the

coherence of the laser.

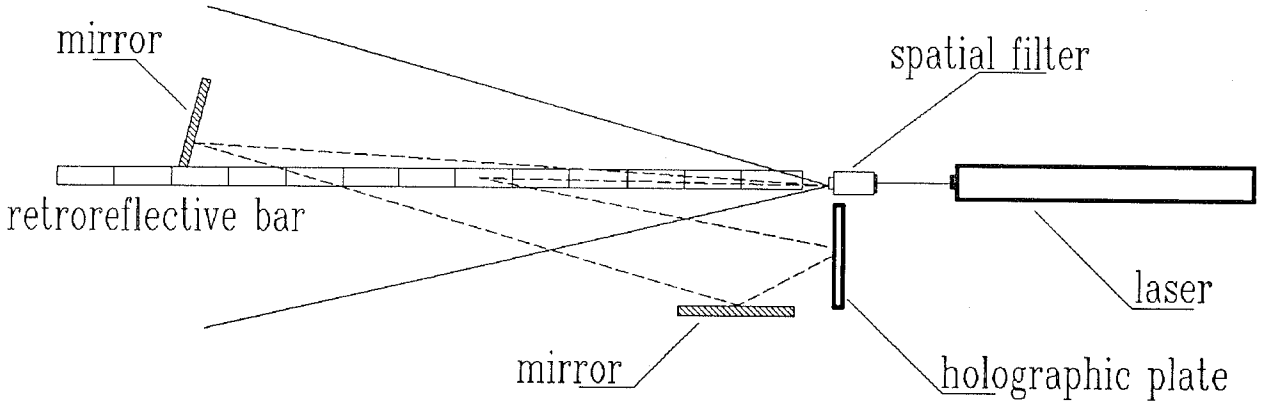

Figure 6

In Figure 6, (a setup first introduced in a paper by a group at Hughes Research Laboratories), a one or two meter piece of metal angel iron is used as the object. It is covered with 3-M Brand Scotchlite contact paper. This product has many tiny glass spheres coated on it which retroreflect incident light. It is important to use this kind of coating, as the bar is illuminated at almost grazing incidence and most of the light would be lost to specular reflection even if the bar were painted with the most diffusely reflecting paint. The laser beam is spread out with a short focal length lens, e.g. a 40X or 60X objective. The coherence length bar is placed in the illuminated field, almost parallel to the axis of the spreading cone of light. The holographic plate holder is placed next to the beam-spreader so as to catch as much as possible the retroreflected light heading back into the spatial filter. A zero path length point on the bar should be initialized, typically the far end. The reference mirror reflects some of the light missing the bar back to the plate holder through another mirror (used to increase the angle of reference so that viewing the hologram will be much easier). Agfa 8E75 holographic plates are used in doing coherence length tests with the He-Ne lasers.

II. Results and Interpretations

Several holograms have been made with both setups and the measurements from the setup in Figure 5 are shown in the table on the next page.

It is interesting to notice that the SP125 and the JEA 1576, though quite different in length, have the same coherence length. This does not agree with the idea that longer lasers have shorter coherence lengths, which many people take for granted.

It is easy to explain this with Equation (12). When the number of modes N within a profile is much larger than 1, the coherence length is proportional to cavity length L, and approximately proportional to the reciprocal of N. But we also know that with the same width of profile (which is true for the SP and the JEA according to Equation (5)), the number

Make (He-Ne)	Output Power (mw)	Cavity Length (cm)	Coherence Length (cm)
Spectral-Physics 125 (without etalon)	45	200	30
Spectral-Physics 125 (with etalon)	8	200	400
JEA HN-1576	13	70	30
Spectral-Physics 138p	1.2	26	105

of lasing modes N is proportional to cavity length L. So coherence length remains nearly the same for these two. The following equation gives an estimate of N using Equations (5) and (7).

$$N = \frac{\Delta\nu_{1/2}}{\Delta\nu_m} \approx 8.76 * L \tag{16}$$

where we have assumed T=300K, A=20, c'=c. For SP125, L=2m, N=18; for JEA1576, L=0.7m, N=6.

In general, combining Equations (12) and (16), we have

$$l_{co} = \frac{2L}{8.76 * L - 1} \tag{17}$$

Here L is the cavity length in meters. Figure 7 shows the dependence of l_{co} on L.

We took pictures of the mode structures of lasers from an oscilloscope when we made the coherence holograms. Based on these mode structures, we can predict the coherence length of the laser under investigation and compare to the measurements. Here are the mode structures and coherence calculations for various lasers:

(i) Spectral-Physics 125 (without etalon)

The mode structure has visible profiles among inevitable noise. It is impossible to evaluate accurately the number of modes. The measured coherence length agrees with common sense and experience. Approximately 18 modes contribute to this short coherence according to Equation (14). If we substitute 18 for N in (12), we get coherence length of 23.5cm, which is not very far from the 30cm coherence measured.

(ii) Spectral-Physics 125 (with etalon)

This mode structure has two adjacent modes within the spectral profile. If 2 is substituted for N into Equation (12), l_{co} = 400 cm, which is in very good agreement with the measured value. The experiment itself may have an error of ±15cm. From the hologram, we can observe a periodicity which appears when there are two modes existing. But the pattern almost completely fades out after two periods. This is because the modes are not as sharp as δ-functions, instead they is broadened as can be seen from

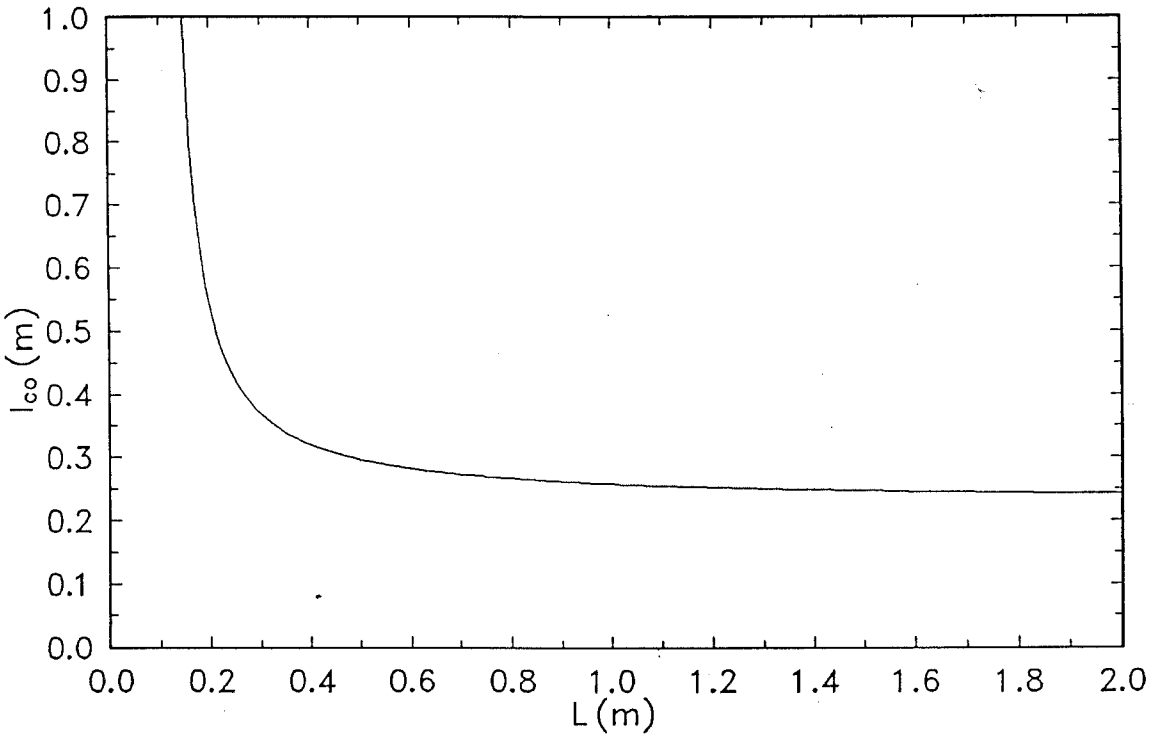

Figure 7

the picture taken with a F-P scanner. This contributes to the attenuation of the intensity. Comparing this to the interferogram in Figure 7 (detected intensity I versus mirror displacement in a Michelson interferometer), we see it fits perfectly.

(iii) JEA HN-1576

The mode structure of this laser has several modes under the Doppler profile. According to the picture of the mode structure, the number of modes within the FWHM of the Doppler profile is 6, which is the same as we calculated from Equation (14). If N is 6 in Equation (12), l_{co} = 28 cm. It is in good agreement with the measured 30 cm coherence, considering experimental errors.

(iv) Spectral-Physics 138p

Within the resolution of the oscilloscope, this laser seems to give single mode. This helps to explain the fact that its coherent length is more than four times the length of its cavity. The simplified models above would give infinity for l_{co} in this case, which is true if each single mode is a δ-function, but in reality each mode has a finite width and it is this width that limits the coherence length of a single-mode laser. The width may be read from an oscilloscope by using an acoustic optical modulator.

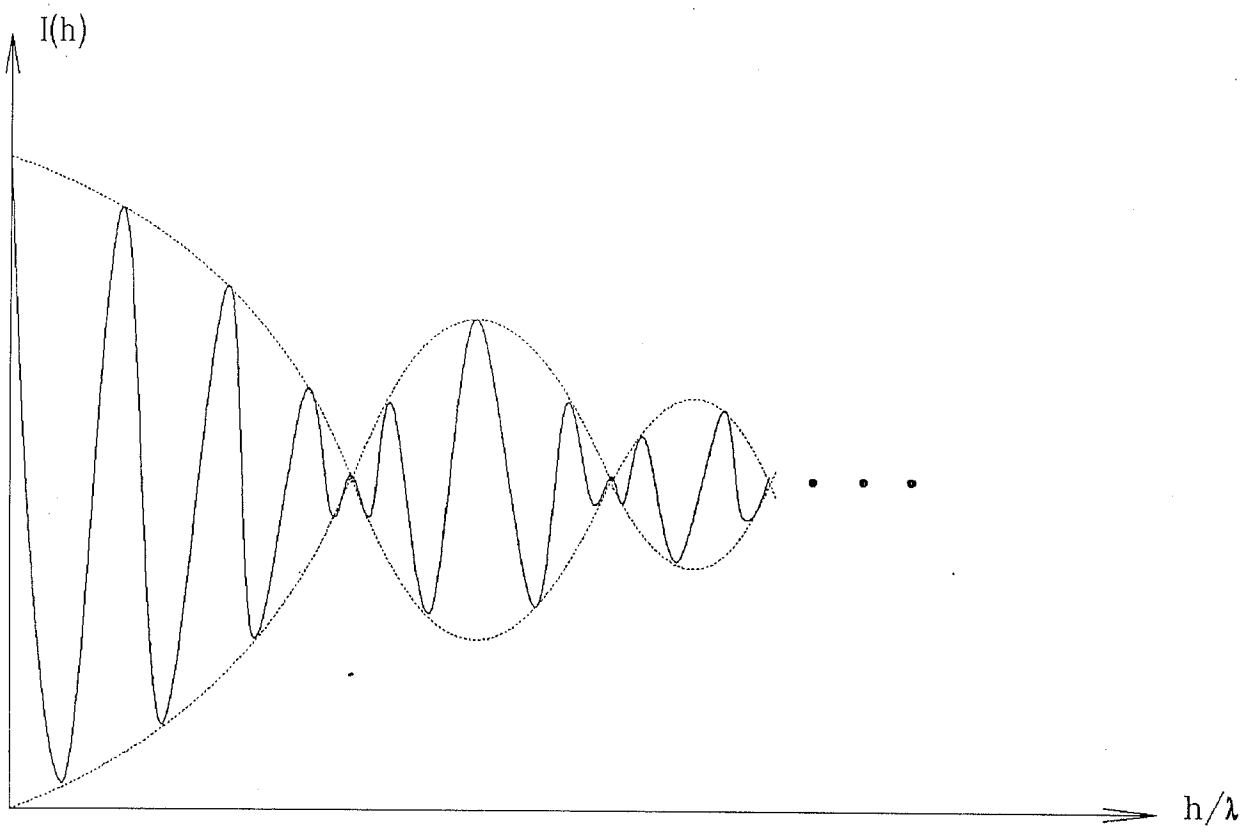

Figure 8

5. An Outline of a Formal Analysis

In order to describe and calculate coherence in a more general and realistic form, we introduce the autocorrelation function $\Gamma(\tau)$ of an analytic signal $\mathbf{u}(t)$

$$\Gamma(\tau) = \langle u(t+\tau)u^*(t)\rangle \tag{18}$$

It is the inner product of $\mathbf{u}(t)$ and $\mathbf{u}(t+\tau)$, also known as the self coherence function of optical disturbance. The normalized self coherence function is called the complex degree of coherence

$$\gamma(\tau) = \frac{\Gamma(\tau)}{\Gamma(0)} \tag{19}$$

The character of an interferogram is determined by $\gamma(\tau)$. The coherence function is the Fourier transform of the power spectral density of the source

$$\gamma(\tau) = \int_0^\infty \hat{g}(\nu)\exp[-i2\pi\nu\tau]d\nu \tag{20}$$

where $\hat{g}(\nu)$ is the normalized spectral density

$$\int_0^\infty \hat{g}(\nu)d\nu = 1 \tag{21}$$

This is the Wiener-Khinchin theorem.

Coherence time can be defined in terms of the complex degree of coherence

$$\tau_c = \int_{-\infty}^{\infty} |\gamma(\tau)|^2 d\tau \tag{22}$$

The calculations we did earlier for the simplified models with continuous spectral density are made with this definition. We now calculate laser coherent length with the more realistic model in Figure 1. Since

$$\textit{normalized Gaussian function} \qquad \hat{g}(\nu) = \frac{2\sqrt{ln2}}{\sqrt{\pi}\,\Delta\nu_G} \exp[-(2\sqrt{ln2}\frac{\nu-\nu_G}{\Delta\nu_G})^2]$$

$$\textit{normalized Lorentzian function} \qquad \hat{g}(\nu) = \frac{2(\pi\Delta\nu_L)^{-1}}{1+(2\frac{\nu-\nu_L}{\Delta\nu_L})^2} \tag{23}$$

where ν_G and $\Delta\nu_G$ are the center frequency and the FWHM for a Gaussian distribution respectively, ν_L and $\Delta\nu_L$ bear the same meaning for a Lorentzian distribution. Assuming each single mode has the same line width $\Delta\nu_L$, the power spectral density may be written as (not normalized)

$$g(\nu) = \sum_{n=-(N-1)/2}^{(N-1)/2} \exp[-a^2(\nu_n-\nu_G)^2] \frac{1}{1+b^2(\nu-\nu_n)} \tag{24}$$

where

$$a = 2\sqrt{ln2}\frac{1}{\Delta\nu_G}, \quad b = \frac{2}{\Delta\nu_L}, \quad \nu_n = \nu_G + n\Delta\nu_m \tag{25}$$

By the definition in Equation (20), the complex degree of coherence may be calculated as follows

$$\gamma(\tau) = \frac{\sum_n p(n)\exp(-\frac{2\pi}{b}|\tau|)\exp(-i2\pi nd\tau)}{\sum_n p(n)} \exp(-i2\pi\nu_G\tau) \tag{26}$$

where

$$d = \Delta\nu_m \quad \textit{and} \quad p(n) = \exp(-a^2n^2d^2) \tag{27}$$

and the coherence time is calculated according to Equation (22).

They all depend on $\Delta\nu_l$, which has a theoretical lower bound limited by Schawlow-Townes equation. But in reality, because of fluctuation and mode drifting, this theoretical limit is not attainable. In our case, we can actually use the this model to estimate the width of single modes.

If an acoustic optical modulator is used, we will be able to tell the scale on the oscilloscope in F-P scanning so that we can actually read the width of each single mode and therefore compare the calculation here with the measurement.

$$N: odd \qquad \tau_c \approx \frac{1+2\sum_{1}^{(N-1)/2} p(n)^2}{\left[\sum_{n=-(N-1)/2}^{(N-1)/2} p(n)\right]^2} \frac{1}{\pi} \frac{1}{\Delta\nu_L}$$

$$N: even \qquad \tau_c \approx \frac{\sum_{m=1}^{N-1} p\left(\frac{m}{2}\right)^2}{\left[\sum_{m=1}^{N-1} p\left(\frac{m}{2}\right)\right]^2} \frac{1}{2\pi} \frac{1}{\Delta\nu_L} \tag{28}$$

$$N=1 \qquad \tau_c = \frac{b}{2\pi} = \frac{1}{\pi}\frac{1}{\Delta\nu_L} \approx \frac{0.318}{\Delta\nu_L}$$

$$N=2 \qquad \tau_c = \frac{b}{4\pi} + \frac{b}{\pi(4+b^2+d^2)} \approx \frac{b}{4\pi} = \frac{1}{2\pi\Delta\nu_L} \approx \frac{0.159}{\Delta\nu_L}$$

$$N=3 \qquad \tau_c \approx \frac{b}{2\pi}\frac{1+2\exp(-2a^2d^2)}{[1+2\exp(-a^2d^2)]} \approx \frac{0.119}{\Delta\nu_L} \tag{29}$$

$$N=4 \qquad \tau_c \approx \frac{b}{4\pi}\frac{\exp(-\frac{a^2d^2}{2}) + \exp(-\frac{9}{2}a^2d^2)}{[\exp(-\frac{a^2d^2}{4}) + \exp(-\frac{9}{4}a^2d^2)]^2} \approx \frac{0.087}{\Delta\nu_L}$$

6. Conclusions

In this paper, we have studied several simplified models of laser spectral density and measured laser coherence holographically. The measurements agree very well with the prediction of Equation (12). A more realistic model has also been investigated, but the results are not directly applicable. At this stage, we recommend Equation (12) as an elegant solution for a quick estimate of coherent lengths of lasers.

7. Appendix

The coherent length equation (12) can also be derived through basic geometric consideration. Figure 9 shows the interference pattern of two identical light sources A and B, which have a spectrum of two wavelengths λ_1 and λ_2 ($\lambda_1 > \lambda_2$). Each wavelength gives rise to a unique interference pattern. The curves depict the constructive superposition of the waves and are hyperbolic. Since there are two wavelengths, the contrast of interference pattern varies periodically in space. The contrast has its maximum on the line bisecting the straight line joining A and B. It gradually diminishes as we move away from the center. When we reach the hyperbola on which C is located, the constructive interference of λ_1 coincides with the destructive interference of λ_2. Hence the contrast is zero. According to our definition of coherence, which is the maximum optical path difference at which interference pattern is recognizable, coherence length is twice the path difference between (AC) and (BC) in this case.

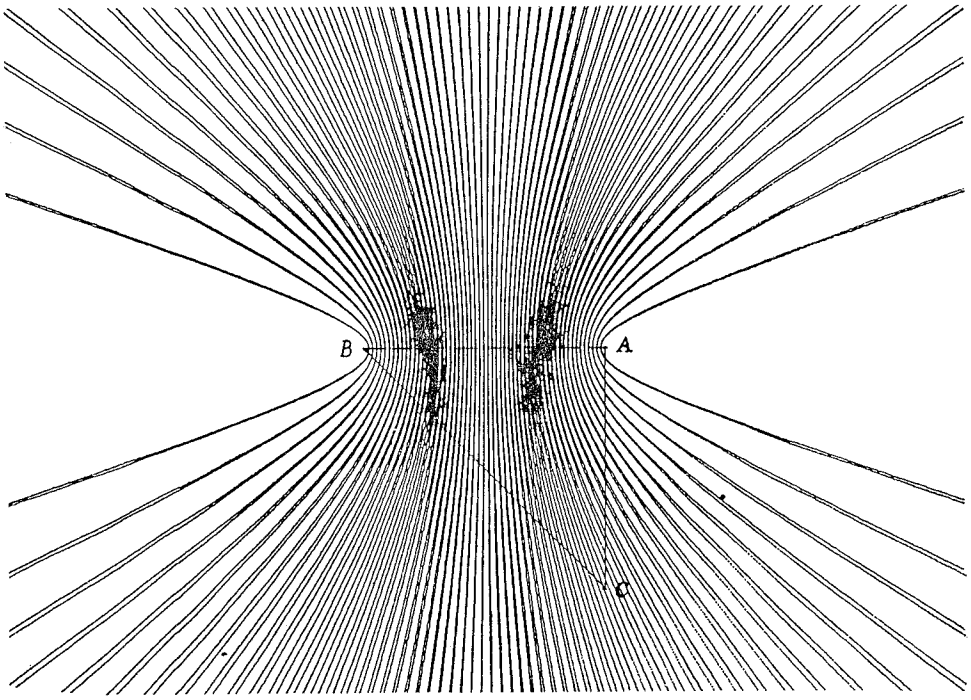

Figure 9

Let $\lambda = (\lambda_1 + \lambda_2)/2$, $\Delta\lambda = \lambda_1 - \lambda_2$, and assume $\lambda >> \Delta\lambda$. The optical path difference ΔL between (AC) and (BC) at which contrast disappears can be calculated as

$$\Delta L = (BC) - (AC) = m\lambda_1 = (m+1)\lambda_2 \tag{30}$$

where m is an integer, and it is easy to see that

$$m = \frac{\lambda}{2\Delta\lambda} \tag{31}$$

Therefore

$$\Delta = \frac{\lambda^2}{2\Delta\lambda} \tag{32}$$

and

$$l_{co} = 2\Delta L = \frac{\lambda^2}{\Delta\lambda} \tag{33}$$

Now let us consider a laser cavity with two resonance modes whose wavelengths are λ_1 and λ_2 as above. Figure 10 shows the standing wave states of the modes. Obviously,

$$L = n\frac{\lambda_1}{2} = (n+1)\frac{\lambda_2}{2} \tag{34}$$

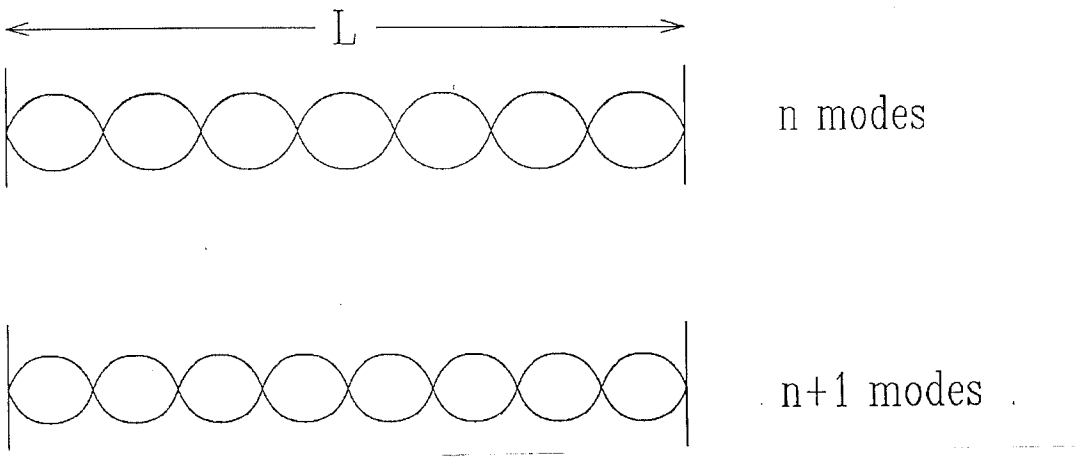

Figure 10

where L is the cavity length and n is an integer. L can be expressed in terms of λ and $\Delta\lambda$

$$L = \frac{\lambda^2}{2\Delta\lambda} \tag{35}$$

Therefore, for a two-mode laser, the coherent length is

$$l_{co} = 2L \tag{36}$$

It can be shown that, for a three-mode laser, $l_{co}=L$, and in general

$$l_{co} = \frac{2L}{N-1} \tag{37}$$

where N is the number of resonance modes.

8. References

1. Corney, A., Atomic and Laser Spectroscopy (Clarendon Press - Oxford, 1977), p. 232
2. Corney, p. 234
3. Corney, p. 248
4. Corney, pp. 251-253
5. Maitland, A., and Dunn, M. H., Laser Physics (John Wiley & Sons, Inc. - New York, 1969), p.103
6. Maitland, pp. 260-266
7 Goodman, J., Statistical Optics (John Wiley & Sons, Inc. 1985), pp. 164-168
8. Goodman, p. 160
9. Goodman, pp. 161-164